Efficient laser polishing of silica micro-optic components

Krzysztof M. Nowak, Howard J. Baker, and Denis R. Hall

We report a study of the basic characteristics of laser polishing of fused silica with a protocol that is particularly suitable for surface smoothing of micro-optic elements fabricated by a laser ablation process. We describe a new, to our knowledge, approach based on scanning a highly controlled small size laser beam and melting areas of tens to hundreds of micrometers of glass using a computer-controlled raster scan process, which does not require beam shaping, substrate preheating, or special atmospheres. Special test samples of silica substrates with prescribed spatial frequency content were polished using a range of irradiation conditions with the beam from a well-controlled CO_2 laser operating at a wavelength of 10.59 μm. An analysis is presented of the laser-generated reduction in surface roughness in terms of measurements of the spatial frequency characteristics, and the results are compared with the predictions of a simple model of surface-tension-driven mass flow within the laser-melted layer. This technique is shown to be capable of smoothing silica surfaces with ~1 μm scale roughness down to levels <1 nm with no net effect on the as-machined net surface shape, at realistic production rates without a preheating stage, and with noncritical residual stresses. © 2006 Optical Society of America

OCIS codes: 000.2190, 220.4000, 220.5450, 120.4610, 120.5820, 350.3390.

1. Introduction

There is continuing interest in the use of lasers to initiate localized softening or melting of thin layers at the surface of silica and other glassy substrates. Such laser processing has been used to produce surface polishing of optical elements in glass[1] and silica,[2] and to inhibit subsequent growth of laser-generated damage,[3] or to repair localized damage sites in silica laser optics.[4] Most work has focused on the use of a carbon dioxide laser because of the moderate reflectivity (~20%) and very high absorption coefficient at the 10.59 μm laser wavelength ($\sim 10^5$ m^{-1}), coupled with the capacity to produce fine control of the spatial and temporal properties of the laser beam. The earliest reported work on CO_2 laser polishing of fused silica is believed to be carried out by Temple *et al.*[5] They investigated the reduction of optical damage threshold (sustained previously by irradiation with nanosecond 1064 nm laser pulses) produced by a CO_2 laser treatment of mechanically polished silica surfaces. The experimental technique was based on the use of a cw laser with a large TEM_{00} spot (8 mm $1/e^2$ diameter) scanned across the substrate surface with a translation speed of ~5 cm s^{-1} and irradiance in the range of 0.3–0.6 kW cm^{-2}. The moving laser spot created a traveling red-hot zone with a dwell time of <1 s, producing a substantial increase in laser damage threshold in comparison with surfaces prepared by mechanical polishing only. A key concern in laser surface processing of glassy materials is the susceptibility to cracking. However, in the work reported in Ref. 5, polarimetric measurements were also carried out and the surfaces were observed to exhibit negligible residual strain following appropriate multipass laser treatments.

The thermal stress limitations imposed on laser polishing of optical glasses were studied by Xiao and Bass,[6] who investigated laser smoothing of a number of glasses including Zerodur, BK-7, Pyrex, and fused silica. Their experimental technique was similar to that used in Ref. 5, but with the important addition of an oven, which allowed the samples to be preheated to 400 °C prior to laser irradiation. They showed that it is the thermal expansion coefficient at the melt temperature that mainly determines the ability of glasses to resist cracking during and after laser treatment. Only fused silica and Pyrex have been successfully polished at room temperature, and these glasses have the lowest expansion coefficient among the materials tested. Subsequently, Laguarta *et al.*[1] and Vega *et al.*[7] carried out an extensive study on the

The authors are with the Department of Physics, School of Engineering and Physical Sciences, Heriot-Watt University, Edinburgh EH11 4AS, United Kingdom. K. M. Nowak's e-mail address is k.m.nowak@hw.ac.uk.

Received 29 March 2005; revised 4 August 2005; accepted 4 August 2005.

0003-6935/06/010162-10$15.00/0

application of CO_2 laser beams for polishing of bulk optics fabricated from conventional glasses such as K or BK crowns. In their experiments, cracking was avoided by preheating the samples uniformly to a temperature near the glass strain point (viscosity 10^{14} Pa s, 400–750 °C for most conventional optical glasses[8]), which reduced the buildup of thermal stress during and after laser polishing. A large nearly flat-top-shaped beam was used to irradiate the glass surfaces with irradiance in the range of 50–235 W cm^{-2} and processing times from 0.4 to 2 s. The authors observed that the time scale necessary for surface flow (within a surface layer of 25 μm depth and with a viscosity of $\sim 10^3$ Pa s) to produce the transition from an initial roughness of 1–10 μm (characteristic of the ground surface) to the polished state (1 nm roughness) was less than several tenths of a second. This technique of preheating thus allowed the authors to demonstrate successful laser polishing of optical glasses that would otherwise crack.

The influence of the laser beam intensity profile in producing nonuniformities in the irradiated glass surface morphology was assessed by Ocaña *et al.*[9] They showed that a bell-shaped peak beam intensity distribution leads to the development of significant temperature variation across the surface, which may be critical since the viscosity of glasses is strongly temperature dependent, falling by approximately 1 order of magnitude per 100 °C temperature rise. They noted that short pulse irradiation with a nonuniform beam spatial profile may create local melt zones of viscosity low enough to produce mass flow under surface tension within the time scale of the pulse, thus introducing unwanted surface modulation with the spatial frequencies of the beam nonuniformity.

All the work outlined so far revolves around the use of lasers for the polishing of bulk optics. In contrast this paper presents to our knowledge the first analysis of performance and applicability of the use of CO_2 laser irradiation for the surface polishing of micro-optic components fabricated in fused silica. In related work, a novel laser machining technique has been developed for the fabrication of custom silica micro-optic elements and successfully applied to the production of micro-optics for the improvement of beam quality of high-power diode laser arrays.[2] The corrective phase plates as produced by this laser machining process are characterized by surfaces of arbitrary shape with roughnesses of approximately 1 μm peak to peak with a period of typically 10 μm, thus giving rise to undesirable scattering of light. Thus there is a need for a postmachining surface treatment, which would eliminate the residual surface roughness and restore the optical quality of these devices. Since the surfaces of the phase plates are nonspherical, polishing by traditional mechanical means is not feasible and other methods would have to be employed, such as electron beam polishing[10] or hydrogen flame plasma jet.[11] This provided the motivation for the current paper, since the laser-based polishing technique is a natural capability of our laser fabrication facility and does not require any additional arrangements, such as costly vacuum technology or special atmospheres.

In this paper we report the achievement of good quality optical surfaces fabricated by a computerized laser processing workstation, using well-controlled pulses from a planar waveguide CO_2 laser and a high-precision X–Y translation table. In Section 2, an analysis of the basic characteristics of the laser polishing process is presented. The residual surface roughness, which is an indicator of the effectiveness of the polishing process, is described in terms of the attenuation in roughness as a function of spatial period and/or frequency. In addition, the key process parameters are identified and practical approaches to controlling them are proposed. In Section 3, the main features of the laser polishing process are confirmed by experiment in a long-pulse mode, using a purpose-designed pulse burst from the laser system. This investigation involved the use of specially designed silica test samples that were used to determine the spatial frequency spectrum of the surface roughness attenuation produced by laser smoothing. Practical polishing protocols, tailored to the realistic pulse generation capabilities of CO_2 lasers are reviewed in Section 4, with a view to producing an economically usable polishing technique for the smoothing of micro-optic components.

2. Surface-Tension-Driven Surface Relaxation

The use of laser irradiation to reduce the surface roughness of glassy materials such as silica requires a laser-induced surface layer temperature increase to the point where melting or at least softening occurs. This then allows surface-tension-driven mass flow within the viscous molten and/or softened layer, followed by resolidification and the elimination of many of the surface imperfections caused by the original mechanical polishing or laser ablation machining. Reference here to the heating of only a surface layer is justified in the case of irradiation with a CO_2 laser at 10.59 μm because the penetration depth (at room temperature) is only ~30 μm. The objective is to produce reduced scattering losses in the laser fire-polished surface. In this laser heating process the avoidance of both surface cracking and the loss of material by evaporation are key requirements. Cracking may be avoided in laser-melted silica, as pointed out in Ref. 6, because of its combination of low thermal expansion at the melting point and its high mechanical strength. Moreover, evaporation may be effectively avoided[12] by ensuring that the glass surface temperature does not exceed 2700 °C.

At this stage, it is necessary to gain some insight into the mass flow dynamics to design and interpret meaningful laser polishing experiments. We assume a thin layer of laser-melted silica, located on top of a solid unaffected substrate. It is clear that the flow properties of this thin film depend on its thickness and material composition, the temperature of the molten material, the time profile of heating, and the

feature height and pattern density of the irregularities (roughness) in the surface topography. We will see that the characteristic time scales for laser polishing in a melt zone defined by the beam parameters can be estimated with the aid of a theoretical model. A simple model has been proposed by White *et al.*[13] who were interested in the planarization of glass surfaces by the viscous flow of borophosphosilicate glasses on planar silicon substrates. Such glass layers provide interlevel insulation for microelectronic structures, where smooth surfaces and the removal of sharp edges are requirements to promote good metallization. The model assumes heat-activated Newtonian viscous flow with the driving force provided by the surface tension and the radius of curvature of the contour of the surface irregularity. A simple sinusoidal peak and trough of amplitude, A, and wavelength, λ, is assumed in a melted layer of average thickness h, surface tension γ, and viscosity η. By equating the shear stress force to the viscous force in the molten fluid, it can be shown[13] that the initial undulation amplitude A_i is reduced to a final value A_f after flow time t given by

$$A_f = A_i \exp\left(-4\pi^2 \frac{\gamma}{\eta} h^3 \frac{1}{\lambda^4} t\right). \tag{1}$$

Equation (1) has been derived with the simplifying assumptions of $\lambda > h > A_i$, constant values of surface tension and a constant viscosity value throughout the molten fluid depth h, and an absence of surface tension gradients and gravitational effects.

The authors of Ref. 13 present results of experiments with borophosphosilicate glasses that are in good agreement with the predictions of the model. Here we are interested in the prospect of applying this analysis to ascertain the time scale for silica surface flow under pulsed laser heating. To do so it is necessary to determine appropriate values of η, γ, and h. In the experiments described in Ref. 13, the viscosity η, was determined simply from knowledge of the furnace temperature and h was defined directly by the thickness of deposited glass. The viscosity could also be assumed constant throughout the depth h, since the use of long flow times t (>1 h) assured temperature uniformity of the microstructure.

In the case of laser polishing, however, the temperature distribution is determined by the absorption depth of the laser radiation and the extent of thermal diffusion taking place on the time scale of laser pulse. The temperature distribution in the material evolves during the time of laser heating and the definition of thickness h and viscosity η turns out to be rather more problematic. Fortunately, it is possible to estimate values of the parameters involved for the purpose of further discussion without plunging into a lengthy analysis. The softening point of glass (viscosity $10^{6.6}$ Pa s)[8,14] is regarded as the onset of plasticity. Thus it is plausible to assume that no significant mass flow can occur in the material at that viscosity within the time scale of a few seconds. Since the avoidance of additional (evaporative) material removal is one of the key constraints of the smoothing process, the surface temperature should be kept below 2700 °C,[12] which implies that the minimum value of viscosity η obtainable in the melt would be approximately 10^3 Pa s.[12] The lower limit of depth h is defined by ~4 μm,[15] the absorption length of the CO_2 laser wavelength in silica at high temperature. In our experiments silica slides of 1 mm thickness have been used, thus the upper limit value can be found easily assuming a steady-state 1D heat flux through the thickness of the slide placed on a heat sink at room temperature. A knowledge of the maximum allowed surface temperature of 2700 °C and the temperature at the softening point of silica (1600 °C)[8,14] allow us to conclude that the upper limit of depth h is ultimately approximately 200 μm. In practice, the pulsed laser irradiation with a millimeter range spot size generates a significantly smaller melt depth as a result of radial heat flow and/or insufficient time for development of a steady-state condition. Melt depth variations in the range from approximately 4 to approximately 100 μm can be produced practically by an appropriate laser spot diameter and irradiation settings. It is probable that the lack of available data on surface tension values for silica in the literature can be explained by the high temperatures needed to carry out such measurements. However, a representative value of γ of 300 mJ m−2 can be used as a reasonable estimate from the convergence of surface tension data for binary silicate glasses.[14]

An intermediate value of thickness $h = 50$ μm and average viscosity of $\eta = 10^5$ Pa s have been selected and used to calculate the spatial frequency response of laser polishing, according to Eq. (1). The results of the calculations are presented in Fig. 1, which shows a predicted evolution of the ratio A_f/A_i as a function of spatial frequency ν (period, λ) at different durations of the melt lifetime with values of 1 μs, 1 ms, and 1 s. Note that the simple model does not include the evolution of melt depth during the laser heating. The strong dependence of the transfer function A_f/A_i, on the spatial frequency as predicted by the model is rather striking. Figure 1 shows that high-performance low-pass filter behavior is expected, with a quite sharply defined cutoff frequency. This extraordinary selectivity is of great significance for the polishing process since it allows controllable removal of high-frequency (roughness) patterns without any net modification of the underlying desired shape.

The time scale necessary for a tenfold decrease of the amplitude of typical postmachining surface roughness (1 μm peak to peak at a spatial frequency of 100 lines/mm) ranges from milliseconds upward. The order of the calculated time scale is consistent with experimental observations made previously by other researchers[1,7] on laser polishing of glasses. From the characteristics in Fig. 1 it is clear that submicrometer features can be highly attenuated in a

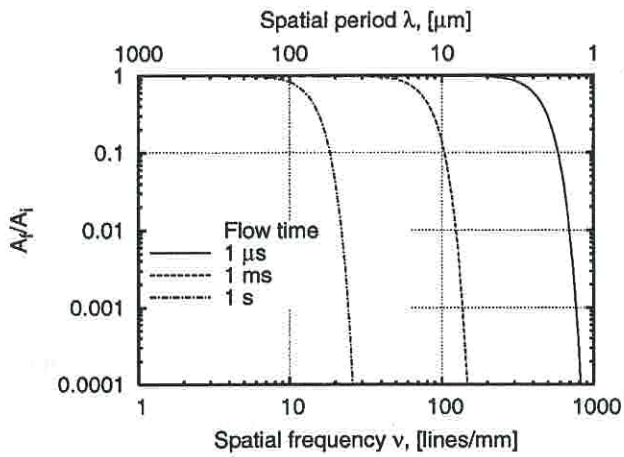

Fig. 1. Theoretical prediction of the frequency response of laser-activated polishing of fused silica at different durations of melt lifetime. Calculated using Eq. (1) with melt depth $h = 50$ μm, average viscosity $\eta = 10^5$ Pa s, and a representative value of surface tension $\gamma = 300$ mJ m^{-2}. Temporal evolution of temperature distribution in the material is not taken into account.

matter of microseconds by surface-tension-driven mass flow. The polishing mechanism described by this model is thus also responsible for the exceptional smoothness of ablation craters produced in fused silica by CO_2 laser pulses.[12] The presence of thin layers (~3 μm) of highly mobile glass (viscosity $<10^2$ Pa s) following CO_2 laser ablation of silica combined with the flow time of the order of microseconds, determined by the cooling rate at the ablation site, results in highly effective polishing action.

The characteristics of surface-tension-driven smoothing of surfaces are determined by the material properties, such as viscosity, surface tension of liquid silica, melt zone dimensions, and the melt lifetime. The advantage of using a laser for polishing is that spatiotemporal parameters, melt zone dimensions, and dwell time can be easily controlled by laser beam settings and the laser wavelength. The beam diameter sets a feature size limit on the polishing process by confining the melt zone area. From the characteristics, shown in Fig. 1, it is clear that the melt zone diameter can be made comparable to the feature size limit (~100 μm) without significantly affecting the polishing mechanism at a first approximation. This localized micropolishing approach allows for a substantial reduction in the laser power necessary to carry out the smoothing process in comparison with previously reported laser polishing, leading to a much lower heat load imposed on the micro-optic component and excellent capabilities for process control. Additionally, uniformity of the laser beam profile is no longer an issue,[9] since the polishing action is confined to a small subaperture area of the polished element. The overall irradiance uniformity can be assured by the overlap of many such areas in a raster scan protocol instead of using costly beam-shaping optics.

The laser can also control the material viscosity, exploiting the strong temperature dependence of this variable simply by delivering the correct amount of heat into the melt zone. The melt depth, determined primarily by the absorption length α^{-1} for CO_2 wavelengths can be controlled to some extent by the thermal diffusion taking place in the area irradiated by the beam. Thus a melt depth in the range of ~4–100 μm can be produced by laser spot diameter and irradiation time adjustments. Another advantage of the method is that any tendency toward devitrification can be suppressed due to the short lifetime of the melt zone. Finally, the predicted smoothing performance can be directly verified by measuring the spatial frequency response with laser beam settings and dwell time as parameters.

3. Initial Experiments: Laser Polishing on Millisecond Time Scales

The purpose of the experiments described in this section was to verify the predictions of the transfer function of the polishing process using laser pulses of the millisecond range. The hardware requirements of such experiments are well satisfied by the laser workstation developed especially for fabrication of custom corrective optics for high-power diode laser arrays,[2] and illustrated by the schematic diagram in Fig. 2. The laser source is an rf discharge-excited planar waveguide CO_2 laser stabilized on the P20 line at 10.59 μm capable of an average power output of approximately 100 W with a discharge-pulsing frequency up to ~10 kHz, with pulse lengths in the range of 5–500 μs and with an M^2 value of <1.2. The laser beam is coupled into a germanium acousto-optic modulator (AOM) that provides pulse duration and intensity adjustment control. The silica samples were mounted on a traveling (*X–Y*) stage system with 0.1 μm resolution, and the laser firing and AOM control were synchronized within the software controlling the table motion. The system operates in a standard laboratory environment without precise temperature or air quality control.

Although the laser is capable of producing millisecond pulses at a duty factor up to 50%, a combination of 500 μs length and 100 Hz pulse repetition frequency (PRF) was chosen as a compromise among long-pulse duration, high PRF, and power output instability of less than a few percent. The 500 μs raw laser pulse has been arranged as a pulse burst consisting of two functional parts: a preheating pulse and a train of micropulses with an adjustable duty factor, as shown in Fig. 3. The duration of the preheating pulse was chosen to be 100 μs as a compromise between good control over melting and the maximum length of the pulse train (400 μs), which was the active part of the burst.

The preheating pulse was designed to quickly raise the surface temperature to a point where substantial surface-tension-driven mass flow could be activated. Note that the depth of melt can also be controlled to some extent by the duration of the preheating pulse. From our previous research we know that significant

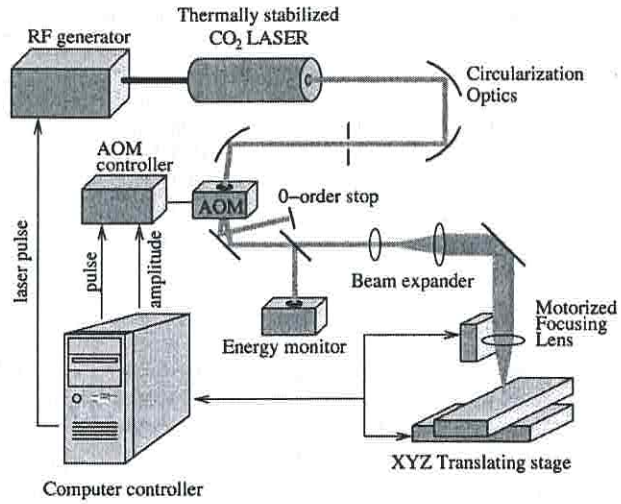

Fig. 2. Schematic diagram of the precision laser machining station used for polishing experiments.

heat dissipation takes place in the material on a time scale of hundreds of microseconds and the melt depth in a range of tens of micrometers can be expected. The task of the train of short pulses within the burst was to maintain a high surface temperature without exceeding 2700 °C, to avoid undesired material loss.

The energy fluence of the preheating pulse and the duty factor of the micropulses were found experimentally for the best smoothing effect without unwanted material removal. Due to the irradiance limit of the laser and the value of material melting threshold at 100 μs of the preheating pulse, the largest laser beam spot size available was 400 μm ($1/e^2$ diameter). Irradiation of the material with such a spot size produced melt zones of 90 μm diameter as shown in Fig. 4.

Initial pilot experiments on laser polishing of abraded silica surfaces had shown that to get meaningful results in the spatial frequency domain, it is necessary for the laser polishing to be performed on test samples with a well-prescribed surface containing the spatial frequency spectrum of interest. Thus the test piece should contain spatial frequencies in the range of 2–500 lines/mm, which is the transition region between residual machining marks and design shape of the optical element produced by laser ablation.[2] The boundaries of the spatial frequency domain have been dictated by the tip radius (2.5 μm) of the DekTak profiler used and the maximum anticipated feature size that should remain unaffected by laser polishing (>100 μm).

Such test samples have been computer generated and written into fused silica substrates by our laser machining system described in Section 3. Figure 5 shows a micrograph of the test sample and its measured surface profile prior to laser polishing. All laser polishing experiments described in this paper were carried out on identical test surfaces that facilitated comparison between different polishing protocols. The nature of the method allowed also for detection of material removal by comparison of sample profiles prior to and after laser smoothing. Fast Fourier transform (FFT) analysis with a Gaussian data window has been applied to the measured spatial profiles to calculate the spatial frequency response for each test surface. Frequency aliasing effects have been avoided since the tip of the profiler acted as an antialiasing filter for the chosen spatial sampling of ~1 μm, highly attenuating the features smaller than the tip radius of 2.5 μm.

The experiments were conducted in such a way that numerous test samples were polished with a number of different duty factors, and the resultant laser polished profiles were measured and subjected to a spatial frequency analysis and examined for undesired material removal. The table motion and pulse timing were arranged such that the melt zones overlapped in a single line on a 10 μm pitch to cover a large area of the test surface to facilitate profiling with the DekTak. The benefit of the overlap was the increase of melt lifetime by a factor of 9 from 400 μs (pulse train duration) to 3.6 ms, thereby shifting the process toward a millisecond polishing time scale where good polishing performance was expected. This accumulated melt lifetime, denoted as t_{acc}, is of interest because it is equivalent to the flow time t from Eq. (1). To avoid heat carryover between the individual melt

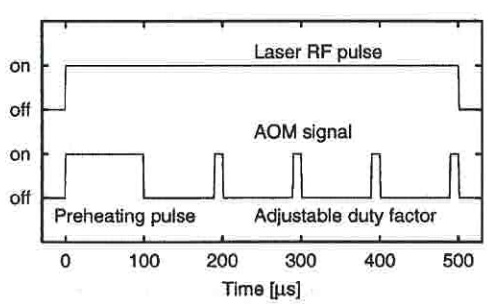

Fig. 3. Pulse burst used for millisecond laser polishing. The preheating pulse is followed by the pulse train. The energy of the pulse train was controlled by adjusting the duty factor.

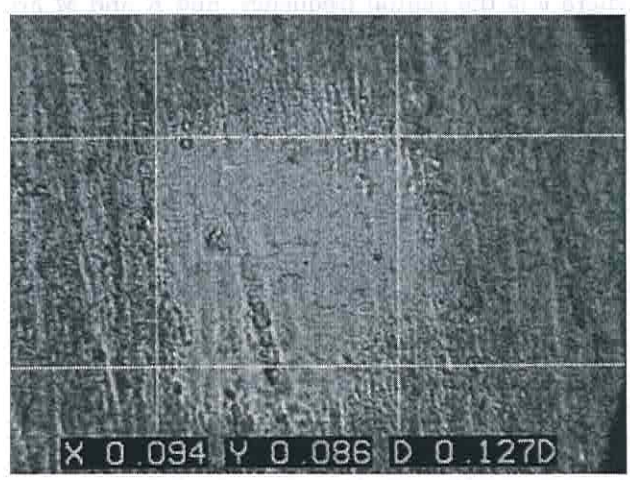

Fig. 4. Micrograph of a melt zone on an abraded surface of a silica slide created by a single pulse of polishing Protocol A. Digital readout in millimeters.

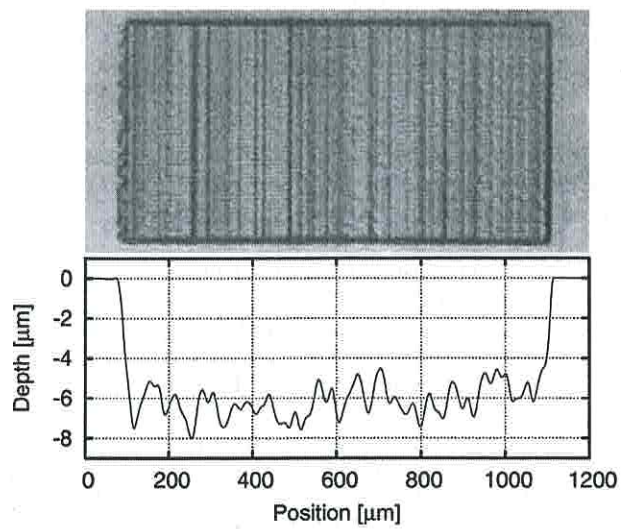

Fig. 5. Micrograph of the test surface used for laser polishing experiments. The dimensions are 1 × 0.5 mm. Below, a typical profile of the test surface before laser polishing.

zones placed on the 10 μm pitch, an interleaving technique has been used, consisting of multipass scanning with sequential laser spot placements 500 μm apart. The results of the search for optimal polishing conditions with single thermally decoupled laser pulses are summarized in Table 1 and designated Protocol A.

The profiles of untreated and laser-polished samples were acquired digitally and analyzed and then used to calculate the spatial frequency spectra, which subsequently enabled calculation of the experimental frequency response characteristics and curve fitting as plotted in Fig. 6. The fitting curve is described by Eq. (2), which resembles the characteristics from Eq. (1),

$$A(\nu) = \exp(K\,\nu^M\,t_{acc}), \tag{2}$$

where ν is the spatial frequency, and K and M are fitting parameters. The values of K and M and their asymptotic standard errors, derived from the optimum curve fit using the Marquardt–Levenberg algorithm, are shown in Table 2. The value of parameter M (predicted to have a value of 4) indicates that the influence of frequency is weaker than predicted by the model, which perhaps can be explained because of the nonuniform distribution of viscosity in the melt layer. Despite this the laser polishing process under these conditions remains effective at removing features of 10 μm scale and below. The parameter K can be used to compare process conditions of different polishing protocols, but the interpretation of its value is of a speculative nature and will not be attempted here. Thus the experiment has demonstrated that laser polishing is capable of substantial smoothing (in the anticipated bandwidth of spatial frequencies) on a time scale of milliseconds without significant material loss. The curve in Fig. 6 resembles the characteristics of a low-pass filter with a cutoff frequency of about 100 lines/mm, corresponding to feature sizes of ~10 μm. To enable comparison of different laser smoothing protocols presented later in this paper, a figure of merit characterizing the laser smoothing process has been chosen as the laser-generated attenuation at a frequency of 100 lines/mm per polishing treatment, A_{100}, and defined as

Table 1. Characteristics of Polishing Protocol A

Protocol Code A	
Spot diameter ($1/e^2$)	400 μm
Melt zone diameter	~90 μm
Pulse burst fluence	10.3 J/cm^2
Melting pulse fluence	6.0 J/cm^2
Overlap of melt zones	10 μm
Acc. melt lifetime	~3.6 ms
Depth removed	<0.1 μm

$$A_{100} = \frac{A_i(\nu = 100)}{A_f(\nu = 100)}. \tag{3}$$

This particular spatial frequency corresponds to the lowest possible undesired spatial frequency introduced by our laser machining system. In engineering terms, A_{100} guarantees that all unwanted roughness of period less than 10 μm will be attenuated at least by the factor specified. In the case of our research, the higher the value of A_{100} the better, since a smaller number of treatments promotes increased process productivity. In practice, there are two ways to boost the value of A_{100}, namely, by increasing the effective dwell time or by elevation of the process temperature by using higher laser energy to produce a less viscous melt. Multiple polishing treatments can simply and safely increase the accumulated melt lifetime, although such an approach compromises productivity. As will be shown in Section 4, better results can

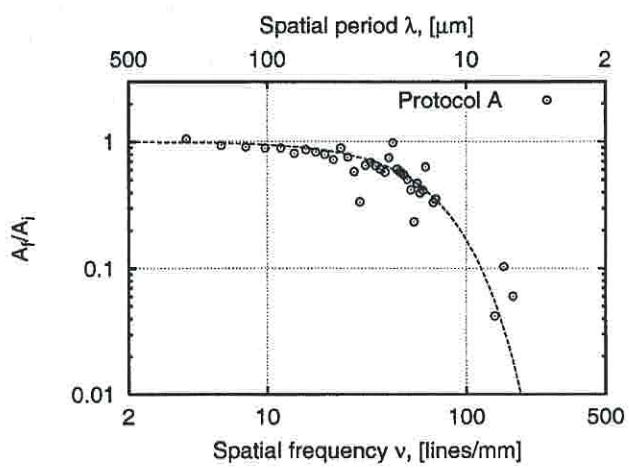

Fig. 6. Frequency response of polishing Protocol A calculated using FFT from the test surface profiles measured with a DekTak profiler. Settings for Protocol A are listed in Table 1.

Table 2. Fitting Parameters for Optimal Frequency Response Curves of Protocols A–D

	Protocol Code			
Fit Parameter	A	B	C	D
M	1.5 ± 0.4	2 ± 0.7	1.6 ± 0.2	1.5 ± 0.2
K	14.7 ± 1.4	1.5 ± 3.3	1.4 ± 0.7	0.9 ± 0.5

be achieved by approaching the limit of 2700 °C. However, it must be kept in mind that working close to the material evaporation temperature increases the risk of undesired material loss and a consequent failure of the polishing process.

For the process developed in this section (specified as Protocol A in Table 1), the value of A_{100} was 2–6 per treatment, and the profile measurements have indicated that the maximum evaporative material loss was less than 0.1 μm. From a wider perspective, this loss ought not to be a problem for optical devices polished in this way provided the minute material loss is uniform across the aperture of the device.

4. Efficient Polishing using High Repetition Rate Pulsing

The potential of laser polishing of as-machined silica surfaces has been demonstrated with pulse bursts incorporating a 100 μs melting subpulse within a burst of duration 400 μs. However, for practical reasons with the available laser system, the PRF of the pulse bursts was limited to about 100 Hz, which restricts the overall processing productivity to an unacceptably low level. This problem has been alleviated by reconfiguring the polishing protocol to function within the practical operating conditions of realistic lasers of a scale suitable for this type of workstation. In contrast to Protocol A, this quasi-cw approach combines raster scanning with a high PRF of 5 kHz and pulses as short as 30 μs. These settings, which were chosen as a compromise between high average power and stable laser operation, offer not only effective dwell times 2 orders of magnitude longer and larger in melt depth, but also high rates of area coverage of ~16 cm^2 per minute. Following a series of processing tests, a set of specified processing conditions, designated as Protocols B, C, and D, were defined and are listed in Table 3. A set of test samples for each protocol was laser polished with various pulse energies to determine the point of maximum performance without material removal.

By using a spot size of 1 mm diameter, a melt track of up to 200 μm width could be created by overlapping the laser shots on a high-density raster pattern. By sequential overlapping of such tracks, an accumulated melt lifetime of hundreds of milliseconds could be achieved, promising high attenuation for micrometer-sized features. This has been confirmed by experiment, as indicated in Figs. 7 and 8. Figure 7 shows a comparison of the frequency spectra of unpolished silica test samples with the results of polishing via Protocol C [Fig. 7(a)] and Protocol D [(Fig. 7(b)]. Significant roughness reduction through laser polishing can be seen in each case. In Fig. 8 the measured spatial frequency responses for Protocols B, C, and D are plotted, using the accumulated melt lifetime t_{acc} as a parameter.

Table 3. Characteristics of Polishing Protocols B, C, and D

Protocol Code		B	C	D
Spot diameter ($1/e^2$)	(μm)	800	800	1000
Aver. laser power	(W)	8.3	6.0	8.2
Pulsing frequency	(Hz)	5000	5000	5000
RF duty factor	(%)	17	17	17
Pulse fluence	($J\ cm^{-2}$)	0.67	0.49	0.42
Scanning velocity	($mm\ s^{-1}$)	10	5	5
Melt track width	(μm)	150	150	200
Melt zone lifetime	(ms)	15	30	44
Raster line spacing	(μm)	10	10	10
Acc. melt lifetime t_{acc}	(ms)	225	450	880
Depth removed	(μm)		<0.1	

According to the theoretical considerations outlined in Section 2 and confirmed by experiment, control over the characteristics of spatial frequency attenuation can be achieved in practice by controlling the beam parameters and the accumulated melt lifetime t_{acc}. However, it should be noted that it is the material viscosity that has the most significant effect on the resultant attenuation of spatial frequencies, because of its strong dependence on temperature. The data presented in Tables 4 and 5 provide strong evidence for this statement by revealing the sensitivity of the figure of efficiency, A_{100}, as a function of the laser pulse energy and the t_{acc}. It can be clearly seen from the data in Table 4 that the laser polishing is sensitive to the laser energy employed. A laser pulse energy variation of only ~5% can enable the process to cross the line between a success or a failure; thus precise control of the laser energy is required to achieve reliable performance. By contrast, adjustment of the accumulated melt lifetime offers a safer way of tailoring the performance of the process, but at the expense of productivity. A compromise must then be sought for a particular application.

In addition to an assessment of surface smoothness based on an evaluation of the spatial frequency distribution, a more direct method was employed involving a comparison of the optical scattering produced by the as-machined and laser polished surfaces when a visible laser beam is incident. A simple light scattering arrangement was employed, consisting of a He–Ne laser, the beam from which was focused at normal incidence to a spot size of 500 μm diameter on the surface of the silica substrate of interest. The transmitted beam was then allowed to strike a screen that was viewed by a CCD camera. Using this simple setup it was possible to measure the transmittance of the sample, its reflectance, and the fraction of laser power lost through diffraction at the surface patterns with an accuracy of ±1%.

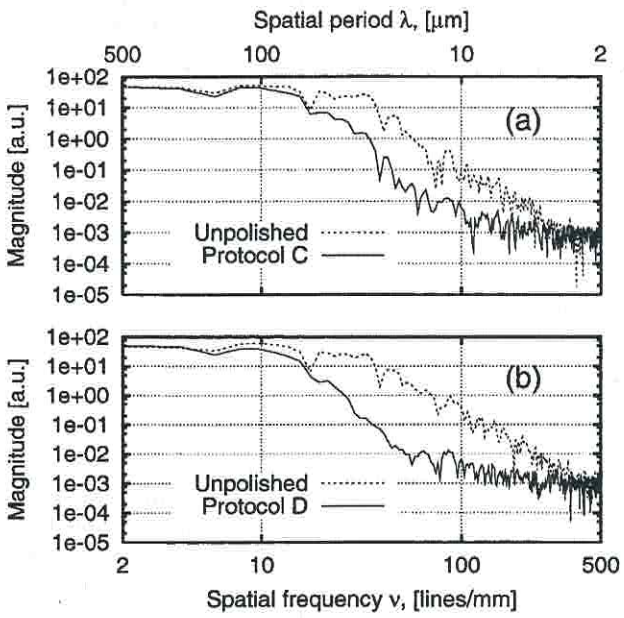

Fig. 7. Frequency spectra calculated using FFT from the test surface profiles measured by DekTak polishing Protocols (a) C and (b) D.

The typical surface of an optical element laser machined by a workstation[2] contains a regular pattern as the result of raster scanning. These micrometer-scale features give rise to efficient diffraction of light transmitted through such a surface. Figure 9(a) shows a typical scatter pattern obtained on the as-machined surface with a raster pitch of 10×10 μm. The bright horizontal and vertical lines correspond to the diffraction on the grating created by orthogonal raster lines. The wide field of laser speckles was a clear indication of the existence of postmachining microdebris.

Next, the as-machined surface was laser polished according to Protocol D (see Table 4) with a fail-safe

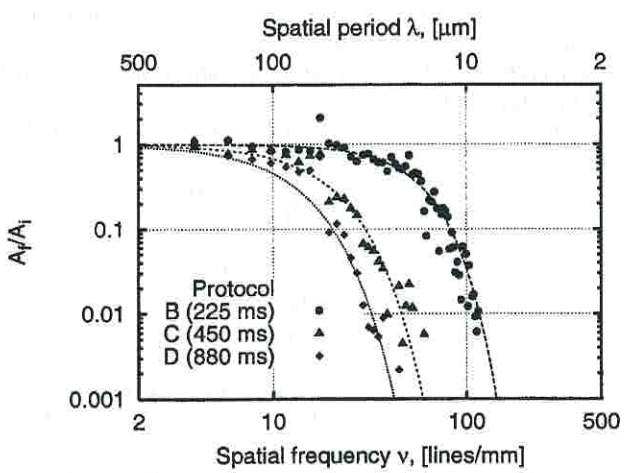

Fig. 8. Comparison of frequency responses of polishing Protocols B, C, and D. The settings are shown in Table 3. A curve described by Eq. (2) has been fitted to the data. Fitting parameters can be found in Table 2.

Table 4. A_{100} versus Pulse Energy: Protocol D

Fluence (J cm^{-2})	A_{100} (Per Treatment)	Depth Removed [μm]
0.38	3–10	<0.1
0.40	17–60	<0.1
0.42	180–560	<0.1
0.44	5600–18 000	0.1
0.47	>100 000	1.1

fluence setting of 0.38 J cm^{-2} and an expected value of A_{100} in the range of 3–10 per treatment. Such a low value of attenuation allowed the observation of incremental polishing action, with a measurable improvement from treatment to treatment. Four consecutive polishing treatments were applied to the same test piece to observe the sequential progress of surface smoothing. Figures 9(b) and 9(c) show the gradual reduction of the intensity of diffraction orders and also of the area occupied by the laser speckles. The first two treatments [Fig. 9(b)] can be seen to have practically removed the microdebris by evaporating it or melting it back into the surface, and the subsequent two treatments [Fig. 9(c)] have continued to reduce the number and intensity of visible diffraction patterns. The significant effect of the laser polishing process can be seen from a comparison of the final transmitted beam profile after the four treatments shown in Fig. 9(c), with the undisturbed reference pattern shown in Fig. 9(d). Scattering efficiency measurements carried out using the setup mentioned above have shown that nearly 50% of the incident laser power was diffracted away from the zeroth order in a form of higher diffraction orders and speckles before polishing. The measurements carried out after the polishing sequence have shown that the transmission was identical to within 1% with the original unmachined silica slide. It must be noted that the polishing raster 1×10 μm did not show up in the diffraction pattern.

Finally, laser-polished samples were evaluated for the presence of postprocess stress and stress-induced birefringence. Test pieces that had been previously laser polished were inspected in a typical polarization measurement setup consisting of crossed polarizers illuminated by a uniform white light source. No detectable differences in appearance and color were observed between the laser polished and the untouched areas. Thus it may be concluded that the optical path difference introduced in a thin layer of laser-affected

Table 5. A_{100} versus Accumulated Melt Lifetime

t_{acc} (ms)	A_{100} (Per Treatment)
3.6	3–10
225	30–100
450	180–560
880	5600–18 000

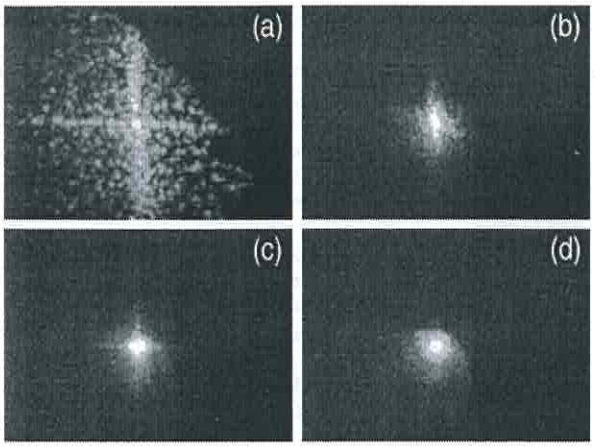

Fig. 9. Photographs showing the transition from high scatter of raw machined surface (a) to lower scatter after (b) two and (c) four polishing treatments. Reference beam (d) shown for comparison.

glass, estimated to be much less than 200 μm, must have been much less than $\lambda/4$, and thus not detrimental to the optical properties of polished devices. However, some evidence of microbending of the substrate (concave upward) has been observed after applying the polishing procedure, and the extent of the bend suggested the presence of residual tensile stress of magnitude about 100–150 MPa. This value is much smaller than the practical strength of relevant glasses[16] of $\sim 10^{-3}\,E$ (E stands for Young's modulus), and postprocess cracking does not occur. Although not detrimental to the optical properties, stresses of this magnitude could create distortion, which might be fatal for precision devices ($<\lambda/4$) with millimeter-range aperture size and a high aperture-to-thickness ratio; thus additional conventional annealing stages may be appropriate in such cases. From the point of view of our applications, however, the microbending mentioned here does not pose a significant problem and has been ignored. Summarizing, it is reasonable to say that the CO_2 laser polishing of silica produces birefringence-free annealed surfaces of excellent optical quality.

5. Conclusions

We have reported an experimental investigation of polishing by laser-heat activated, viscous mass flow, which has exhibited a high degree of consistency with theoretical predictions, based on a simplified flow model reviewed in Section 2. The anticipated low-pass spatial filter characteristics have been verified and confirmed experimentally. The model can also explain the excellent smoothness of crater walls produced in silica by CO_2 ablation machining. It has been shown that the CO_2 laser can also be used to produce efficient removal of the micrometer-scale surface patterns introduced by methods of laser fabrication of micro-optic devices in fused silica. Raster scan laser polishing of silica has been shown to be capable of restoring the optical quality of as-machined surfaces (fabricated by laser ablation) without additional surface modification. This technique not only offers high productivity rates of $>16\ \mathrm{cm}^2$ per minute but also provides operational simplicity and excellent process control. All important process parameters, including melt zone dimensions, polishing time, and material viscosity can be controlled (though not always independently) by simple selection of the laser beam parameters. Moreover, there is no need for expensive beam-shaping optics and the process can be carried out in air at atmospheric pressure and at room temperature. It is shown that the reduced melt zone area used in this approach, compared to conventional laser polishing employing large beams, results in significantly reduced heat load on the treated optical elements and lower laser power requirements.

The process described here requires only one or two laser polishing treatments with appropriate laser beam characteristics to attenuate surface roughness of a 10 μm period or less, and amplitude of ~ 1 μm by more than 3 orders of magnitude. The representative polishing protocol employed a near TEM_{00} beam of 1 mm diameter, PRF of 5 kHz, a pulse duration of 30 μs, and fluence of $0.42\ \mathrm{J\ cm^{-2}}$ combined with a raster scanning on pitch of 1×10 μm. In addition, the laser-polished surfaces were observed to be free of cracking and stress-induced birefringence.

Further improvement in this laser-polishing technique can be expected by the use of a laser wavelength with a smaller optical absorption coefficient in silica. Lower absorption would allow for deeper melt and for faster temperature distribution buildup, as compared to thermal conduction in the case of higher material absorption. This would increase the productivity of the laser-polishing process.

Scattering measurements have shown that laser-generated surface smoothing is such that practically no difference is observed between the laser polished surfaces and the untreated silica optical surface, and measurements have also confirmed that the laser-polishing protocol does not contribute to diffraction from the treated surfaces. The unavoidable postprocess tensile surface stresses are well below practical strength of relevant glasses and do not cause either cracking or significant birefringence, but may be of concern due to the microbending of the substrate. In such cases, a conventional annealing procedure may be required to restore the precise original shape of the element.

References

1. F. Laguarta, N. Lupon, and J. Armengol, "Optical-glass polishing by controlled laser surface-heat treatment," Appl. Opt. **33**, 6508–6513 (1994).
2. J. F. Monjardin, K. M. Nowak, A. R. Holdsworth, H. J. Baker, and D. R. Hall, "Brightness improvement for micro-lensed, laser diode bar stacks," presented at Advanced Solid-State Photonics Topical Meeting, San Antonio, Tex., 2–5 February 2003.
3. R. M. Brusasco, B. M. Penetrante, J. A. Butler, and L. W. Hrubesh, "Localized CO_2 laser treatment for mitigation of damage growth in fused silica," presented at the Boulder Laser Damage Symposium XXXIII, Boulder, Colo, 1–3 October 2001.
4. E. Mendez, H. J. Baker, K. M. Nowak, F. Villarreal, and D. R.

Hall, "Highly localized CO_2 laser cleaning and damage repair of silica optical surfaces," presented at the Boulder Laser Damage Symposium XXXVI, Boulder, Colo, 20–22 September 2004.
5. P. A. Temple, W. H. Lowdermilk, and D. Milam, "Carbon-dioxide laser polishing of fused-silica surfaces for increased laser-damage resistance at 1064 nm," Appl. Opt. **21,** 3249–3255 (1982).
6. Y. M. Xiao and M. Bass, "Thermal-stress limitations to laser fire polishing of glasses," Appl. Opt **22,** 2933–2936 (1983).
7. F. Vega, N. Lupon, J. A. Cebrian and F. Laguarta, "Laser application for optical glass polishing," Opt. Eng. **37,** 272–279 (1998).
8. D. G. Holloway, *The Physical Properties of Glasses* (Wykeham Publications, 1973), pp. 19–20.
9. J. L. Ocaña, A. Garcia-Beltran, F. Laguarta, J. Armengol, N. Lupon, and F. Vega, "Laser heat treatments driven by integrated beams: role of irradiation nonuniformities," Appl. Opt **38,** 4570–4576 (1999).
10. J. Hentze and V. Lissotschenko, "Method and device for the production of optical lenses or the like," U.S. patent 5,504,302 (2 April 1996).
11. V. P. Veiko, "Laser-based technology for micro-optics and photonics components fabrication," in *International Symposium on Photonic Glass*, C. Zhu, ed., Proc. SPIE **5061,** 103–111 (2003).
12. G. A. J. Markillie, H. J. Baker, F. J. Villarreal, and D. R. Hall, "Effect of vaporization and melt ejection on laser machining of silica glass micro-optical components," Appl. Opt **41,** 5660–5667 (2002).
13. L. K. White, N. A. Miszkowski, W. A. Kurylo, and J. M. Shaw, "Flow properties and contour modeling of fusible borophosphosilicate glasses," J. Electrochem. Soc., **139,** 822–826 (1992).
14. A. Paul, *Chemistry of Glasses* (Chapman & Hall, 1982), pp. 75, 88.
15. A. D. McLachlan and F. P. Meyer, "Temperature dependence of the extinction coefficient of fused silica for CO_2 laser wavelengths," Appl. Opt. **26,** 1728–1731 (1987).
16. L. Holland, *The Properties of Glass Surfaces* (Chapman & Hall, 1966).